Article

Effects of Tunnel-Soil-Structure Interaction and Tunnel Location on the Seismic Response of Steel Structures

Arash Rostami

Department of Civil Engineering Islamic Azad University, Central Tehran Branch, Tehran, Iran, Dr.arash.rostami@gmail.com

Abstract: Research shows that in earthquakes the ground response changes in areas where there are underground cavities. Due to the fact that subways and underground tunnels pass from beneath buildings in urban areas, these changes in ground response have a direct impact on the seismic behavior of structures. In this study, first by model validity and reliability of the results, steel structures modeling was conducted and steel structure behavior was evaluated due to Tunnel-Soil-Structure seismic interaction. Parameters studied are number of stories, soil type, tunnel depth, horizontal tunnel-structural distance and dynamic loading. Considering that one of the most important parameters of structural control is drift and story displacement, so this important factor will be considered. The results show that tunneling has a direct effect on the rate of structural displacement and increases the structural response. Also, the behavior of the structure is affected by the position of the structure at the ground level and the position of the tunnel and this should be considered during the design phase of the structures.

Keywords: Seismic Interaction, Tunnel-Soil-Structure, Steel Structures, Drift, Seismic Response

1- Introduction

Nowadays it can be seen that in megacities, traffic and transportation problems could not be solved on the ground surface. Past experience has revealed that the best and fastest way to solve urban transportation in populated areas is to use underground structures. The main phenomena of underground excavations are ground surface displacement, tunnel surrounding displacement and earthquake acceleration changes. Nowadays underground structures such as tunnels, Metro stations and underground parkings are vital infrastructures in most megacities. For many years it was thought that underground tunnels were safe structures and showed an appropriate performance in earthquakes, but in recent earthquakes a lot of tunnel failures have been reported from these underground structures [1-3]. This was more tangible in shallow underground structures; in between what has mainly attracted the attention of researchers is the destruction and damage to the surface structure due to the magnification of surface response which is affected by the presence of these underground spaces [4-12]. In this regard Tabatabaei fard et al. studied on the simplified structure and soil interaction method and presented an equation for evaluating the research results [13]. On the other hand Abat and et al concentrated on modeling and numerical analysis of the structures' seismic response in the tunnel and said that the settled tunnel in soil causes shrinkage throughout the tunnel [14-15]. Pitilakis et al. assessed the circle tunnel effects on the ground surface response and behavior and acceleration changes, and presented that the presence of circle tunnels causes acceleration changes on the ground surface.

In this regard, several scientists such as Osmarini, Wang, Mitra, and Sagar [16-19] focused on changes in Earth's acceleration. On the other hand, Rostami et al. looked at the amount of force applied to the wall of underground tunnels, and concluded that most internal force was applied on rectangular tunnels [20-21]. Tsinidis et al. Investigated the effect of rectangular cavities in soft soils by numerical and laboratory methods. The study suggested that numerical models may produce more accurate results by considering all the uncertainties involved in the problem that rectangular tunnel responses have recorded in centrifuges [22].

Baziar et al. focused on the ground surface seismic response using physical modeling with shaking table and centrifuges [23]. Fatahi and Tabatabaeifar studied on the seismic behavior of structures on soft soil and did not study further and mainly concentrated on soft soil behavior. The results of this research indicated that the differences between the calculated base shear by equivalent linear method and fully non-linear method were not remarkable [24]. Regarding asymmetry at ground level, Rostami et al. studied the response of ground surface in sloped ground and stated that the amount of response in upstream and downstream slopes was quite different [25]. Numerous efforts have been made in this field, such as the studies of Sika, Rostami, Tsouar, Liu, and Luen [26-34]. Various studies have been carried out to address this issue.

One of the most important points in the study of structures and in the design of structures is the displacement of structure floors or floor drift. In the previous studies, many efforts have been made on the effect of the tunnel on changes in ground acceleration and soil-structure interaction. But a detailed study of Tunnel-Soil-Structure interaction has been undertaken. On the other hand, Tunnel-Soil-Structure interactions focusing on ground-level structures located over buried tunnels have not been studied. Therefore, in this study, a state-of-the-art Tunnel-Soil-Structure model was developed by direct design using the very powerful Abacus software to accurately and precisely achieve the dynamic Tunnel-Soil-Structure interaction. The modeling sample can easily calculate the nonlinear behavior and nonlinear geometry of the structure in dynamic analysis. Due to the application of a completely nonlinear behavior in modeling, nonlinear soil behavior in analyzing the dynamic system of Tunnel-Soil-Structure interaction and any nonlinear structural relationships that may arise for the analysis can be calculated with this type of model.

2- Introducing Parametric Studies

In this study, the effects of parameters such as tunnel depth, frequency content, number of floors, type of structure, distance of structure from tunnel on the seismic response of ground surface structure will be investigated. Figure (1) shows a schematic form of system modeling. As can be seen from the figure, the structure is located on the soil bed in the depth of the tunnel. For detailed review, as mentioned above, various parameters have been changed and the changes of the parameters will be examined for the behavior and response of the structure. In this figure R is the tunnel diameter , D the depth of the tunnel, H the horizontal distance of the structure from the tunnel, S the height of the structure, a the depth of the soil mass, and b the mass of the soil mass, and the input wave is applied to the model bed. Also for a more accurate analysis, parameters were made dimensionless so more accurate results were conducted.

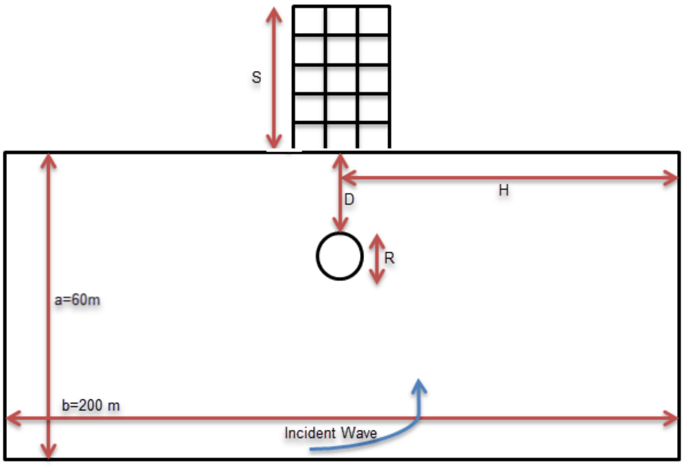

Figure1: Schematic shape of modeling and the soil, structure and tunnel location

In this figure, 20R = b and 6R = a, and in this analysis, dimensional parameters have been used for detailed analysis. These dimensionless parameters include D / R depth to diameter ratio, H / D depth to horizontal distance ratio and S / D tunnel depth to structural height ratio. Also in this study, the Ormsby wavelet was applied to the soil bed and then seven real acceleration mappings were used for applying the earthquake force, which will be describe below.

2-1- Input WAVE

2-1-1-Ormsby Wave

Ormsby waves are one of the zero phase waves that aerospace engineers call it the modified Ormsby wave by applying a wave filter. The modified Ormsby trapezoidal shape in the frequency spectrum can be seen in Fig. (2). An Ormsby wavelet will have many side lobes. Unlike Raker's simple wavelet which always has only two side lobes. The Ormsby wavelet will have a steeper slope than the slope of the trapezoidal filter sides. Four frequencies are required to specify the shape of an Ormsby filter and are also used to identify an Ormsby wavelet (ie, 5-10-40-45 Hz Ormsby wavelet) (fig 2). These frequencies are "fl", low frequency " f2 ", low pass frequency;" f3 ", high pass frequency" f4 ", and high shear frequency are all used in the following formula to produce an Ormsby wavelet. The wave formulation is also presented in Formula 1.

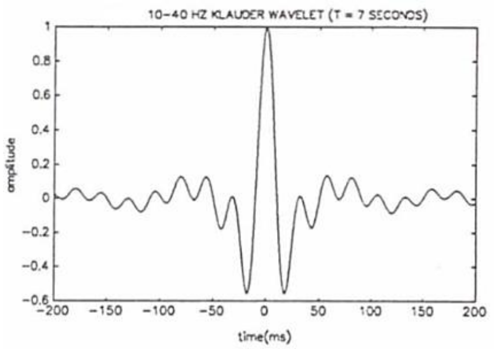

Figure2: Ormsby wavelet shape

$$\text{Ormsby}(t) = \left[\frac{(\pi f4)^2}{\left((\pi f4) - (\pi f3)\right)} \sin^2(\pi f4t) - \frac{(\pi f3)^2}{\left((\pi f4) - (\pi f3)\right)} \sin^2(\pi f3t)\right] - \left[\frac{(\pi f2)^2}{\left((\pi f2) - (\pi f1)\right)} \sin^2(\pi f2t) - \frac{(\pi f1)^2}{\left((\pi f2) - (\pi f1)\right)} \sin^2(\pi f1t)\right] \quad (1)$$

After applying this wavelet to the structure, since the study process is based on the reference article and at first the Riker wave is radiated, in this study because of a larger range of Ormsby wave that covered more wavelengths this wave was used. We used and applied the wave to the model first and then applied the actual mapping acceleration to the model. Since the study is general and aims to determine the structural response to different earthquakes, therefore, based on the soil type, the modeling and its conformity was conducted according to Euro Code earthquake characteristics of these seven real earthquakes based on the Euro Code recommended by this Code, so these records are used in the analysis. For modeling process based on the 2800 Code [35] earthquakes are applied to the soil mass floor (Table 1).

Table1: the characteristics of the seven Euro code earthquakes

Earthquake Name	**Station Name**	**Year**	**Distance of Fault (Km)**	**Magnitude (Richter)**
KOBE	TOT	1995	119	6.9
LOMAPRIETA	Station Gilory	1989	9.64	6.93
NORTHPALM	Silent Station Valley	1986	19.5	6.06
NORTHRIDGE	Station Vasquez	1994	27.7	6.69
PARKFIELD	Temblorpre	1996	11.7	6.19
SANFRANCISCO	Golden gate Park	1957	11.13	5.28
WHITTIERNARROWS	Station Mt Wilson	1987	22.4	5.99

3- Verification and Modeling

This section examines how structures are modeled and the validation for modeling in the Abacus software. Regarding modeling and validation in different softwares, they are described in the following.

3-1- Verification

In this section, we review the model validation based on the reference article [16]. In the validation based on the data of the reference paper [16] carried out with LSDYNA software, the soil behavioral model was Mohr-Columbian and for two-dimensional analysis the plate strain element was used for soil mass. The tunnel is drilled by TBM method and its lining is made of concrete. The information entered is based on the reference article. The model mesh is based on the STRUCTURE command and the mesh size for the tunnel surrounding is selected smaller to calculate more accurate stress values. As can be seen from Figures (3 and 4), the results are very close to the reference article values and the error rate is below 3%, which can be for the differences in software type. It is clear that by getting closer to the surface, the acceleration has increased. Also presented in Figure 5 is an analytical result of the software showing the changes in the ground surface and its magnification.

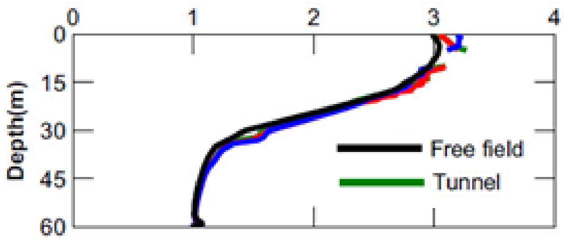

Figure3: the ground surface acceleration diagrams of the reference article [15].

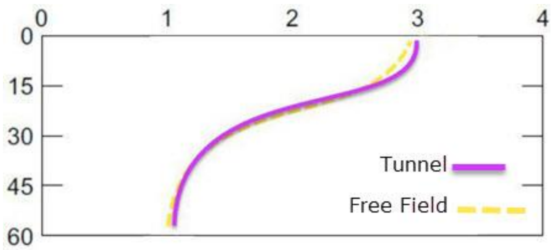

Figure4: the ground surface acceleration diagrams of the validation model

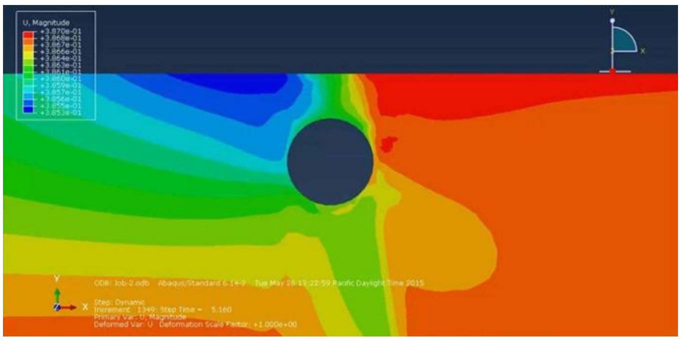

Figure5: A figure of ground surface acceleration changes due to Ormsby wave application

3-2- Steel Structure Modeling

The lateral bearing system of the steel structures used in this article which are located on the soil (Fig. 7) are bending frame and are for (5-10-15) floors. The length and width of the plan is (20) meters and the height of each floor is 3.2m (Figures 6-7) and Table (2) provides information on steel structures. These structures were designed according to ASCE7-05 standard [36] using ETABS software. The analysis for these structures is linear-time-history type so that they are analyzed by earthquake records in a non-tunnel state. The roof structures are block joists weighing (600) kg dead load and (200) kg live load in each square meter. The surrounding walls load are also applied on the side beams for each floor (600) kg/m and for the roof (160) kg/m. for gravity loading the 6th Standard code[37] and for seismic loading the 2800 standard [35] was used. The beam and column sections were chosen from the software by (EURO.PRO) . The sections used in each class are in accordance with Table (3). in Linear and nonlinear time history analysis scaled earthquake records should be used. To scale the records, acceleration mapping coordination is used in accordance with the 2800 standard. In the linear time-history analysis, the obtained base shear is coordinated with the base shear of linear static analysis due to structural standards.

Table2: Size and Dimensions of the Used Frames

Reference Name	Number of Stories	Number of Bays	Story Height (m)	Bay Width (m)	Total Height (m)	Total Width (m)
S 4	4	3	3	4	12	12
S 8	8	3	3	4	24	12
S12	12	3	3	4	36	12

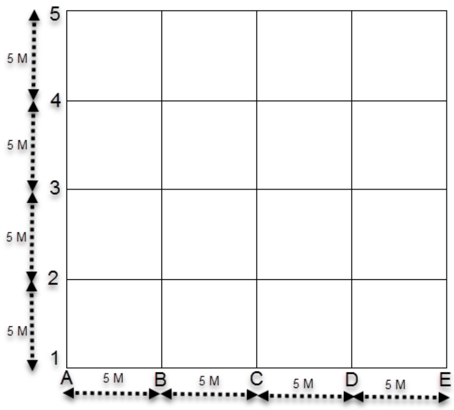

Figure6: 5, 10 and 15 floor steel structure plans

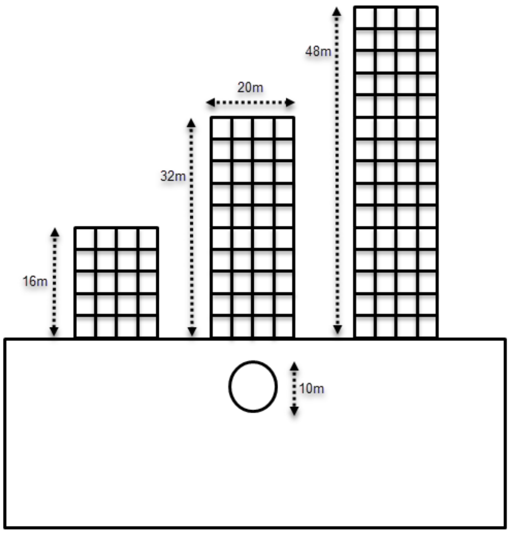

Figure7: 5, 10 and 15 floor steel structures

Table3: the sections used in the steel structure

Num	Structure	Storey	Column	Beam
1	5 Storey	1 & 2	HE280B	IPE270
2		3 & 4	HE260B	IPE270
3		5	HE260B	IPE240
1	10 Storey	1 & 2	H400*237	IPE360
2		3 & 4	H400*237	IPE360
3		5 & 6	HE400B	IPE360
4		7 & 8	HE360B	IPE270
5		9 & 10	HE360B	IPE240
1	15 Storey	1 & 2	H400*744	IPE600
2		3 & 4	H400*744	IPE600
3		5 & 6	H400*634	IPE600
4		7 & 8	H400*634	IPE600
5		9 & 10	H400*340	IPE600
6		11 & 12	H400*340	IPE500
7		13 & 14	H400*237	IPE360
8		15	HE400B	IPE270

3-3- Modeling the soil and tunnel

In this section the tunnel and soil are modeled. In this study the tunnel is excavated using a TBM and the lining of the tunnel is made from high strength concrete which its characteristics is mentioned in table4. The tunnel is assumed to be buried in the ground so that the displacements are applied directly from soil. Also in the tunnel lining modeling Beam elements are used and the tunnel is connected to soil by the Tie command. On the other hand, for modeling the soil, the elastic-plastic or Mohr-Columbian behavioral model is used which are presented in Table 5. The size of the structure is selected according to the reference article, which is 200 meters long and 60 meters wide.

Of course, certain criteria for determining these dimensions have been stated by the researchers, which will be discussed in the following. The mesh size is small enough to allow fine accuracy in the results and also to prevent divergence of the analysis so that the mesh size can easily simulate wave propagation. For this purpose, the dimensions of the elements are smaller than one tenth of the shear wavelength (Δl>λ / 10) propagated in the medium on the basis of the recommendation of Collimer and Lyselmer [38]. The damping value is 5% and Rayleigh damping is used. To prevent the waves from spreading into the soil, the Lysmar Free Field model was used and springs were used to absorb the incoming waves.

Table4: Soil Properties

Depth (m)	soil specific weight (Kn/3³) ϒ	Soil pressure factor K_0	shear wave velocity (m/s) Vs	Daping % D	Poison ratio D	adhesion C Kpa	internal friction angle (degree) φ
0-30	20	0.5	500	5	0.333	20	35
30-40	20	0.5	650	5	0.333	20	45
40-50	20	0.5	700	5	0.333	20	45
50-60	20	0.5	750	5	0.333	20	45

In this table (ϕ) is the internal friction angle, (C) is adhesion, (D) is the Poison ratio. Due to the given factors and the soil specific weight (ϒ), shear modulus (G) and shear wave velocity (V_s) can be calculated. For calculating the shear wave velocity equations (2,3) were used.

$$G = \frac{E}{2(1+D)} \qquad 2$$

$$V_S = \sqrt{\frac{G}{P}} \qquad 3$$

Table5: Tunnel Characteristics

β	α	ϑ	R_{inter}	C	Ø	ψ	E	γ_d	γ_{sat}	L	H
				$kn/_{m^2}$	Degree	Degree	$kn/_{m^2}$	$kn/_{m^2}$	$kn/_{m^2}$	m	m
0.001	0.01	0.3	0.7	0.4	29	5	50000	17	17	200	50

In this table by (d) the covering thickness and (ϒ) the concrete specific weight, the axial rigidity (EA) and bending rigidity (EI) can be calculated by the equations.

4- Effective Parameters In Direct-Soil-Structural-Tunnel Method

In this section, we investigate various factors in modeling and theory of Tunnel-Soil-Structure system. The important point here is to integrate the tunnel system into the soil-structure system. Considering that the tunnel is buried in the soil, the behavior of the tunnel and its displacements and stresses are directly related to the soil mass, so that the Tunnel-Soil-Structure system can be adapted from the direct soil-structure model. So, here are the things to come.

4-1- Introduction

The equations governing the interaction movements of the hybrid structures (soil and structures) and the method of solving these equations are relatively complex. Therefore, the direct method is the method in which the whole soil-structure system is formed in one step, which is used in this study. The use of direct method requires a computer program that can simultaneously discuss the behavior of soil and structures in equal proportions [39]. Therefore, the Abacus finite element software, version 2-14-6, is used to model the structure-soil-tunnel system and to solve complex geometric equations and boundary conditions. The program can simulate a variety of soil and structural behavior models. The materials are provided by elements that can be adjusted to suit the geometry of the model. Each element behaves according to a defined basic model in response to applied forces or applied constraints. To model the structure-soil-tunnel system in a straightforward way, a new advanced Tunnel-Soil-Structure model is designed in Abacus that simulates and analyzes all interactive aspects of the complex dynamical system present in this interaction in a realistic and accurate manner (Figure 8).

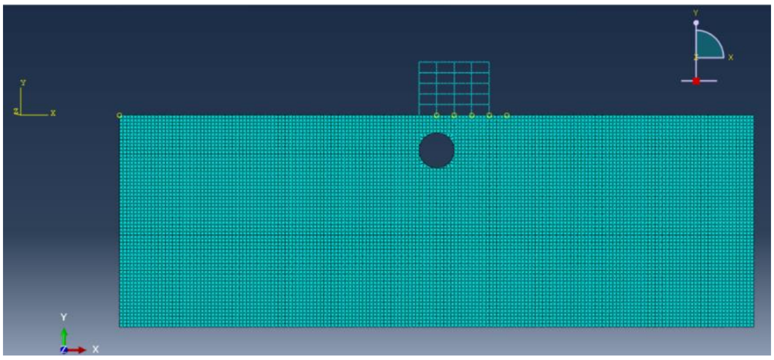

Figure8: Tunnel-Structure-Soil Sample Modeled In Abacus Software
(5-Floor Structure and Tunnel in a 15m Depth)

The structure-soil-tunnel model includes elements consisting of beams for modeling structural components and tunnels, two-dimensional surface strain quadrilateral elements for modeling soil medium, and interface elements for simulating frictional contact between soil and structure and tunnel. The rigid boundary conditions depend on the bedrock and the lateral boundaries of the soil environment are assumed to be viscous boundaries to prevent the reflection of outward propagation waves into the model. The lateral boundaries are attached to the free boundaries on both sides of the model to assume responsibility for the free field motion in the absence of the structure. The various components of the structure-soil-tunnel model are shown in Figure 9. Idealization of structures with composite systems including soil, structures and tunnels as well as boundary conditions are described in the following sections.

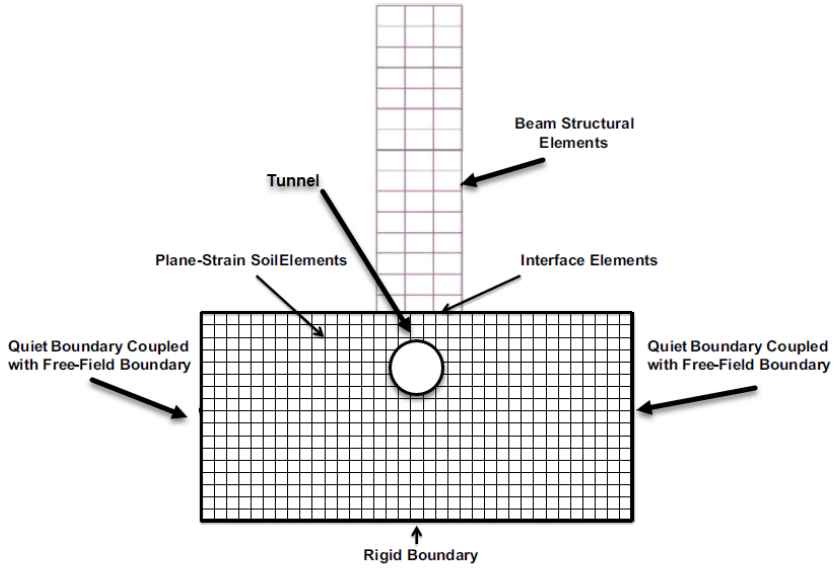

Figure9: Components of the Tunnel-Soil-Structure Model

4-2- Elastic Dynamic Analysis and Design

Workshop civil engineers usually use nonlinear analytical methods for seismic evaluation and design of existing and new buildings. The main purpose of seismic analysis is to accurately predict the expected behavior of the structure against future earthquakes. This has become an important goal with the emergence of a performance-based design (PBD) as a technique for seismic evaluation and design using performance prediction for structural safety and risk assessment [41]. Since structural damage implies inelastic behavior, traditional design and analysis methods are based on linear elastic techniques and can only implicitly predict the level of performance. In contrast, the purpose of the seismic analysis method is to directly estimate the amount of non-elastic and distortion (performance level) changes. Performance levels classify structural states after being exposed to a particular hazard as either 1) fully operational, 2) operational, 3) life safety, 4) near collapse, and 5) collapse. Overall lateral deflection, ductility demand, and inter story drift are the most commonly used damage parameters [42-43]. These five levels of quality performance correspond to the maximum inter story drift (as a damage parameter): 0.2% - 0.5% - 1.5% - 2.5% and more than 2.5%, respectively. Therefore, analysis and seismic design method in this study are directly used to estimate the level of performance of structural system. In structural analysis and design of seismic design, the final load of the structure is considered as the design criterion. This is a fast approach and provides a rational approach to structural analysis. It also provides a cost-effective design because the sections required in this method are smaller in size than the linear method. Also, this method uses a plastic moment to determine the plastic behavior of column and beam elements.

4-3- Structure

Structural elements such as beams, columns, slabs, foundations and tunnel lining are defined using beam elements in the structure-soil-tunnel model (Figure 2). Structural elements of the two-node beam element, finite elements, with six degrees of freedom per node include three transitional and three rotational components. Structural element logic is applicable by explicit solution method. By default, the beam acts as an isotropic, linear, boundless elasticity material; however, a restrictive plastic moment can be specified to shape the structure's rigid behavior. Large displacements, including nonlinear geometrical displacements, can be replaced by the determination of a larger solution; and the complete dynamic response of the system in the time domain can be obtained with the dynamic analysis option. As mentioned earlier, non-elastic structural analysis has been used in this study. The general process of non-elastic structural analysis resembles conventional linear methods in which engineers create a structural model that is then subjected to a predicted earthquake-related motion or external excitation. In this study, the non-elastic bending is simulated by the determination of a finite plastic moment in the structural elements. If a plastic moment is specified, its value can be calculated with respect to a flexible bending structural member with a b width and an h height with yield stress of the material σy (Formula 4). If a composed element member has a perfectly elastic behavior, MP plastic resisting moments for rectangular sections can be calculated as follows:

$$M^P = \sigma_y \left(\frac{bh^2}{4}\right) \qquad 4$$

Where b is the width, h the cross-section height, and σy is the yield stress of the materials. The present formulations used in this study assume that the structural elements behave flexibly until they reach (or become) the specified plastic moment. In the parts where the plastic moment is obtained, they can deform without resistance.

4-4- Soil

The soil environment of the substructure has been simulated using two-dimensional plane-strain networks. In this scheme, the solid soil mass is divided into a finite element network consisting of four elements. The Mohr-Coulomb model in the present study has been used as a constructive model in the structure-soil model to simulate the nonlinear behavior of soil medium and Tunnel-Soil-Structure system. The Mohr-Coulomb model is a complete plastic model developed by many researchers (e.g. [23,45-44]) and has been used to model the effect of structure – soil dynamic interaction to simulate soil behavior at seismic loads in soil – structure – tunnel systems.

4-5- Interface Elements

The foundation location in numerical simulations is separated from the adjacent soil zone by interface elements to simulate frictional contact. The relationship between foundation and soil is modeled using Ks shear springs and ordinary Kn between two surfaces that are in contact with each other using linear system springs. These relationships are defined using the shear failure criterion of the Mohr-Columb failure criterion (Figure 10).

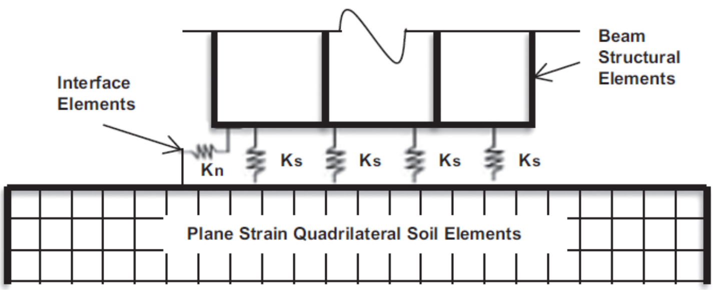

Figure 10- Interface Elements Including the Shear and Normal Spring Stiffness

The relative motion of the interface is controlled by the interface of hard values in normal and tangential directions. The stiffness values of ordinary shear springs for the soil-structure model interface element are set to 10 times the stiffness of the adjacent region. This is based on the relationship recommended by EL Naggar [45] and the Itasca Consulting Group [46] for soils having similar isotropic properties (Formula 5):

$$K_s = K_n = 10\left[\frac{k + (4/3)G}{\Delta z_{min}}\right] \qquad 5$$

Where K and G are the shear and mass coefficients of the neighboring region, and Δzmin is the smallest width of an adjacent region in the normal direction. The current numerical model employs the contact logic defined by Cundall and Hart [47] for both sides of the interface. This code maintains a list of grid points (i, j) located on each side of each specific level. Each point is taken in turn and examined for contact with the nearest neighbor on the opposite side of the interface. During each time step, the velocity (u_i) of each grid point is calculated. Since the displacement velocity units are in the time step, and the calculation of the time step unifies to accelerate convergence. The incremental displacement for any given time is equal to the incremental relative displacement vector at the point of contact is inclined toward the normal and shear components, and the normal shear forces are generally determined as follows:

$$\Delta u_{i=}\dot{u}_{\iota} \qquad 6$$

$$F_n^{(t+\Delta t)} = F_n^{(t)} - k_n \Delta u_n^{(t+0.5\Delta t)} L \qquad 7$$

$$F_s^{(t+\Delta t)} = F_s^{(t)} - k_s \Delta u_s^{(t+0.5\Delta t)} L \qquad 8$$

Where ks is the shear spring stiffness, kn is the normal spring stiffness, L is the effective contact length, Fs is the total shear force and Fn is the total normal force, us is the relative displacement vector in the shear direction and un is the incremental relative displacement vector in the normal direction and Δt is the time step.

4-6- Lateral Boundary Conditions Of The Model

Chopra and Gutierrez [48] proposed that stationary conditions can be assumed at numerical grid points at the lateral boundaries of the soil in the vertical direction, whereas free conditions can be assumed in the horizontal direction. These types of borders are called primitive borders. In the vertical state, free boundaries can be realistically assumed horizontally. However, in dynamical problems, such boundary conditions can reflect the outward propagation waves into the model and do not allow the required energy radiation. In this regard, Roesset and Ettouney [49] proposed an alternative as the best solution to this problem and proposed viscous boundaries to avoid the reflection waves generated by the lateral boundaries of the soil. They concluded this after a comprehensive study of the performance of different types of soil boundary conditions for dynamic problems. Therefore, for lateral boundaries of the soil medium, viscous boundaries have been proposed and developed by Lysmer and Kuhlemeyer [50] for use in this study. The proposed method is based on the use of independent bumpers in the normal and shear directions at the model boundaries. This bumper creates a normal viscosity and shear traction provided by the following formula:

$$T_n= -\rho C_p v_n \qquad 9$$

$$T_s= -\rho C_s v_s \qquad 10$$

In these equations Tn and Tz are respectively normal and shear raction at model boundaries; vn and vs are normal and shear elements at velocity boundaries; ϱ is the density of matter. And Cp and Cs are the wave forms of p and s, respectively. Numerical analysis of the seismic response of surface structures requires the division of an area adjacent to the materials near the foundation. Seismic input (or applied seismic force) is typically propagated by plane waves propagating upward beneath the material. Ground responses that are not affected by the presence of structures are considered as free ground movements. In this study, in the extended structure-soil-tunnel model, the boundary conditions on both sides of the model are considered for the free-field displacement that exists in the absence of the structure. The boundaries of free land have been simulated using an advanced technique that involves performing one-dimensional free calculations in parallel with the main grid analysis.

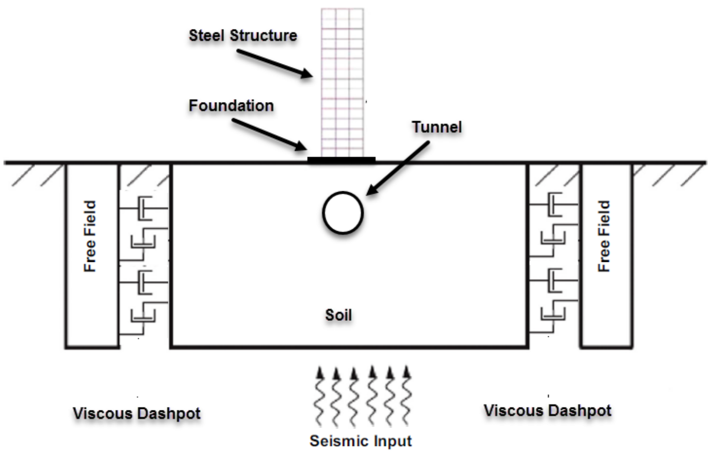

Figure11: Tunnel-Structure-Soil Schematic Shape and Lateral Boundaries

As shown in Fig. 11, the lateral boundaries of the main grid are connected to the simulated free-surface grid by the bumpers, which represent the viscous boundaries on both sides of the model, and the unbalanced forces from the free-field grid are applied to the main grid boundary. Both conditions applied to the left border are expressed as follows:

$$F_x = -\left[\rho C_p\left(v_x^m - v_x^{ff}\right) - \sigma_{xx}^{ff}\right]\Delta S_y \qquad 11$$

$$F_y = -\left[\rho C_s\left(v_y^m - v_y^{ff}\right) - \sigma_{xy}^{ff}\right]\Delta S_y \qquad 12$$

In these equations, F_x and F_y are the unbalanced forces applied to the free land grid towards the main boundary grid in the x and y directions. ΔS_y is the average vertical zone size at the network boundary point. v_x^m is the velocity of the x point of the network in the main network. v_y^m is the speed of the point y in the main grid. v_x^{ff} the velocity of the point x grid on free ground. v_y^{ff} The velocity of the point y of the grid on free ground. σ_{xx}^{ff} is the mean horizontal stress of free land at grid point and σ_{xy}^{ff} is the mean free shear stress at grid point. Also, similar expressions may be written for the right border.

As such, the plane waves traveling upwards do not cause any distortion at the boundary, since the free land network provides conditions similar to those in the infinite model. It should be noted that if the main grid is uniform and there are no surface structures, lateral bumping will not be applied because the free land grid performs the same movement as the main grid.

4-7- The Model bedrock boundary conditions

In terms of bedrock boundary conditions, Kocak and Mengi [51] explained that hard boundary conditions are the most suitable conditions for modeling the main bedrock for dynamic analysis of soil-structure. Dutta and Roy [52] also reached the same conclusion in their critical review of the idealization of the soil-structure system. In addition, in numerical analysis performed by other researchers (e.g. [53-54]) the boundary conditions for the hard bedrock are assumed. According to previous studies, hard bedrock boundary conditions in the numerical model of structure-soil-tunnel have been used in this study. In addition, earthquake acceleration is directly applied to grid points along the hard bedrock of the grid in the present study.

4-8- Soil boundary distances

Concerning the distance between the boundaries, Rayhani and Naggar concluded that the horizontal distance of the lateral boundaries of the soil should be at least five times the width of the structure. In addition, Rayhani and Naggar [45] recommend a 30-meter maximum bedrock depth in numerical analysis after conducting comprehensive numerical modeling and centrifuge model testing, since the highest magnification occurs at the first 30-meter soil level. The horizontal distance of the soil mass is 5 times the width of the building. In addition, modern seismic codes (e.g. [56-41]) only address the effects of location based on features 30 m above the soil surface. Considering that in this study the effects of tunnel depth are also considered, we consider 60 m depth. Therefore, in this study, the maximum bedrock depth is 60 meters, while the horizontal distance of soil boundaries is 100 meters. However, it should be noted that according to Luco and Hadjian [57] when there is deep bedrock, the representation of the three-dimensional soil system interaction with the two-dimensional models can lead to the underestimation of the maximum response.

5- Discussing the results

In this section, the results of modeling are examined. Due to the factors under consideration including the number of floors, tunnel depth, and horizontal distance of the structure from the tunnel, we therefore focus on examining these factors individually and the interaction between Tunnel-Soil-Structure. The studied structures consist of three types of simple bending frame steel with different heights. Also, to investigate the effect of tunnel depth, the tunnel was set at a depth of 10-20-30-40-50 meters and also to investigate the effect of horizontal distance between tunnel and structure of buildings they were located in distances of 5-10-15-20 meters from the tunnel and the effects of this interaction were calculated. In the numerical analysis performed by other researchers on two-dimensional and three-dimensional modeling in soil-structure systems (e.g. [50, 52, 57-58]), the difference between the final results of two-dimensional plane strain and three-dimensional models using artificial rigid bedrock is not remarkable. For example, Seo et al. [57] developed three-dimensional frequency-dependent elements for soil-structure interaction analysis and compared the analytical results of their three-dimensional model with the other three simple two-dimensional models from previous studies. They showed that although good results were obtained using three-dimensional elements, the results of the three-dimensional and two-dimensional analysis were negligible with some conditions such as rigid bedrock. A similar approach has been used in this paper by several other researchers such as Zheng and Takeda [53], Galal and Naimi [59], Tabatabaiefar et al. [60].

5-1- Five-Floor Building

In the modeling, a complete nonlinear time history analysis was used to evaluate the response of the steel structure due to Tunnel-Soil-Structure interaction. In this case, more than 70 analysis were performed for each structure with respect to the number of acceleration records (7 cases) and the number of evaluation modes (5 depth modes and 5 horizontal modes) and the average results have been presented in Fig. 12 (a and b). As shown in Fig. 12a, the horizontal axis is the structural floors and the vertical axis is the structural displacement in centimeters. This figure shows that the tunnel has a direct impact on the movement of the structural floors. A closer look at this figure reveals that the structure at the 5-meter location of the axis tunnel has the highest displacement, meaning that the magnification occurs not at the tunnel axis but at a distance of 5 meters. It is clear from this figure that by distancing from the tunnel axis the tunnel's impact on the displacement of the structure decreases. Fig. 12b shows the amount of drift in the structure as the horizontal axis is based on meter, and as can be seen, the maximum amount of drift has occurred in the structure when the structure is within 5 m of the Tunnel axis and as the structure distances from the tunnel axis this rate decreases. Fig. 13 (a and b) shows the displacement and drift rate of the 5-story structure with tunnel displacement in depth. It is speculated that the tunnel has a direct impact on the displacement and drift of the structure, and on the other hand, this displacement decreases as the depth increases and the maximum displacement is at a depth of 5 m near the surface. The drift amount is calculated according to the standard from Formula 13:

$$drift = (d_{i+1} - d_i)/h \qquad 13$$

Which d_{i+1} is the floor displacement in the (i+1) floor and d_i is the floor displacement in the (i) floor and h is the structure height.

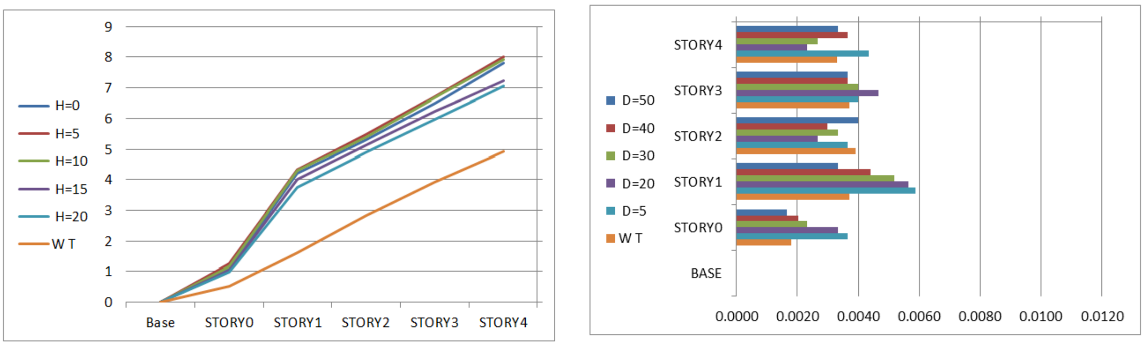

Figure12: Displacement and Drift Diagram of a 5-Story Structure Due To Changes in the Horizontal Distance between the Structure and the Tunnel. The Right-Hand Shape, the Displacement of the Structure; the Left-Hand Shape, Floor Drifts

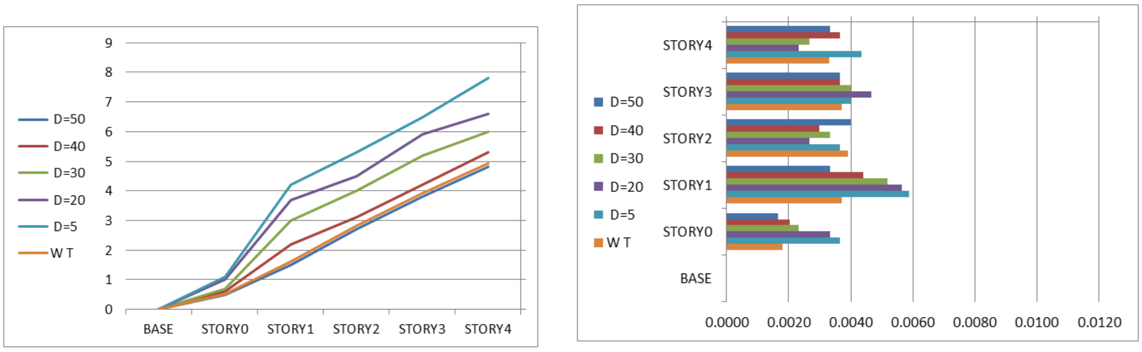

Figure13: Displacement and Drift Diagram of a 5-Story Structure Due To Changes in the Vertical Distance between the Structure and the Tunnel. The Right-Hand Shape, the Displacement of the Structure; the Left-Hand Shape, Floor Drifts

5-2- Ten-Floor Building

The next case is to investigate the tunnel-structure-soil interaction effect of the ten-floor steel structure. As it can be seen from Fig. 14a, the tunnel has a direct effect on the displacement of the structure and the presence of the tunnel causes a change in the displacement of the floors. In the figure where the horizontal axis represents the number of floors and the vertical axis shows displacement in centimeters, it is clear from Fig. 14a and b that the displacement decreases with the distance between the structure and the tunnel increases, meaning that the tunnel is magnified around itself and affects the structural response and by distancing from the tunnel this effect reduces. It is important to note that in the figure the maximum displacement and drift is visible at 5 m from the axis of the tunnel, and that the responses before and after this position are less than this value.

In Fig. 15 the tunnel position changes in depth and the structural response to the tunnel depth changes is shown. As the depth increases its influence on the structural response reaches a minimum and on the other hand the maximum response is presented at the nearest depth to the ground. Thus, a circular tunnel near the surface causes changes in the structural response and affects the behavior of the structure, and as the depth of the tunnel increases, the effect decreases.

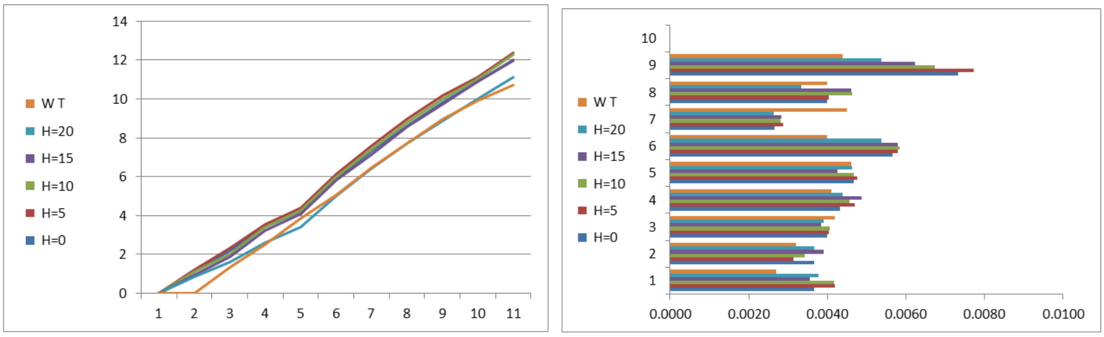

Figure14: Displacement and Drift Diagram of a 5-Story Structure Due To Changes in the Horizontal Distance between the Structure and the Tunnel. The Right-Hand Shape, the Displacement of the Structure; the Left-Hand Shape, Floor Drifts

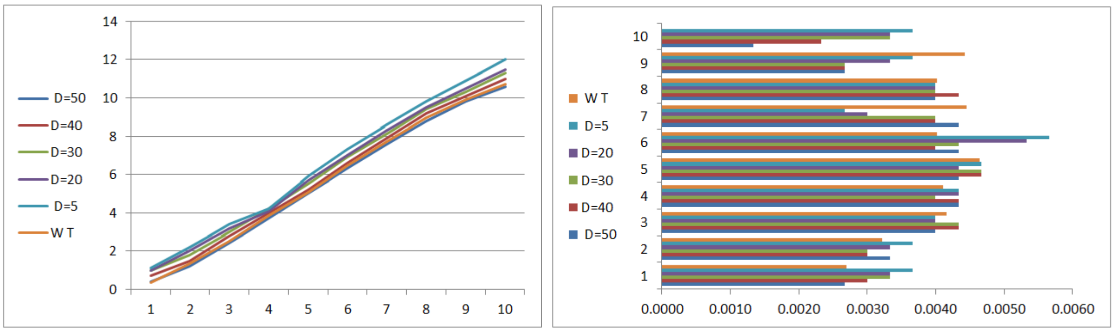

Figure15: Displacement and Drift Diagram of a 5-Story Structure Due To Changes in the Vertical Distance between the Structure and the Tunnel. The Right-Hand Shape, the Displacement of the Structure; the Left-Hand Shape, Floor Drifts

5-3- Fifteen-Floor Building

In the case of the 15-story building, which the effects of a circular tunnel on its seismic response will be evaluated, are shown in Figures 16 and 17. Fig. 16 is related to the displacement of the structure along the horizon and the variation of this parameter in the figure is presented. As seen in the shape, it is quite obvious that the tunnel has a direct effect on the structural response, and this effect is due to the distance between the tunnel and the structure, and the further the tunnel departs from the structure, the lower the effect in Fig. 16 (a and b). It can be clearly seen in the figure that this response reached its maximum within 5 m of the tunnel axis , and among the displacement and drift graph (16b) the highest response was within 5 m between the structure and the tunnel. It is evident in this figure that a tunnel-free structure has less response (displacement and drift) than a tunnel-like structure.

Figure 17 illustrates the structural response to tunnel depth changes. As it can be seen from the figure, that most responses are for the 15-story structure, by an accurate look it could be concluded that the structural displacement and drift are affected by the tunnel depth, as in the other

5 and 10-story structures, and most of the responses are at the nearest tunnel depth. This effect has been reported to decrease as the depth increases, and after the 50m depth it has no effect which correlates with the results of other researchers mentioned earlier, and in fact the magnification happens up to 30 m below ground level.

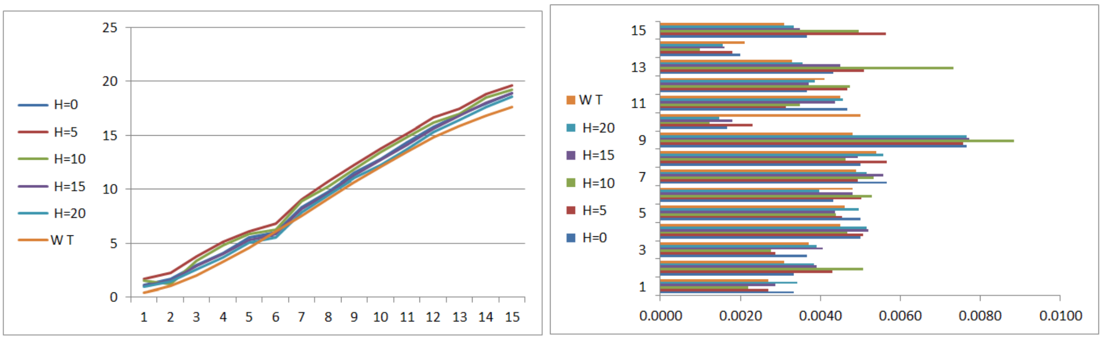

Figure16: Displacement and Drift Diagram of a 5-Story Structure Due To Changes in the Horizontal Distance between the Structure and the Tunnel. The Right-Hand Shape, the Displacement of the Structure; the Left-Hand Shape, Floor Drifts

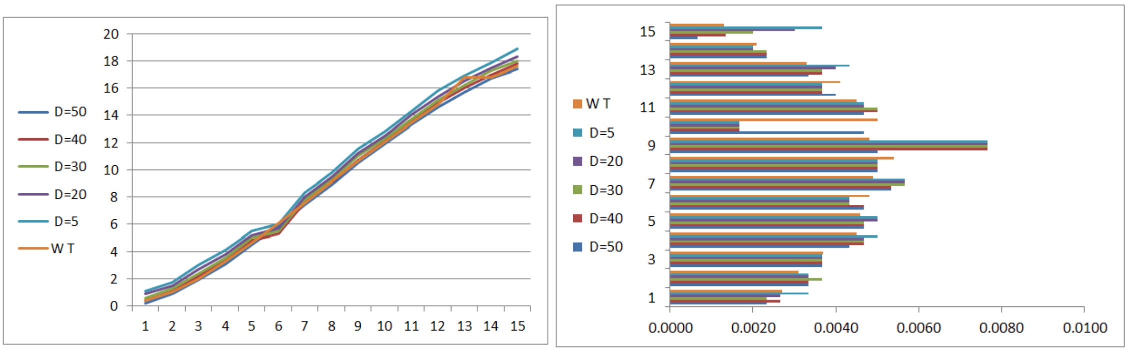

Figure17: Displacement and Drift Diagram of a 5-Story Structure Due To Changes in the Vertical Distance between the Structure and the Tunnel. The Right-Hand Shape, the Displacement of the Structure; the Left-Hand Shape, Floor Drifts

6- Conclusion

In this study, an accurate, complete and state-of-the-art model was modeled in Abacus software to analyze Tunnel-Soil-Structure interactions and was affected by various earthquakes based on Eurocode accelerographs. In this study, parameters such as type of structure, number of floors, depth of tunnel and horizontal distance of structure and tunnel were investigated and the following results were obtained:

- The existence of a circular tunnel changes the surface response and magnification.
- The variation of the ground response due to the circular tunnel is such that the ground surface response at the sides of the tunnel gives greater magnification than the axis and the vertical axis of the tunnel.
- As the depth of the circular tunnel increases, the effect on the surface response decreases.
- The highest ground surface response is observed at the position closest to the ground.
- The further the distance from the tunnel along the horizon, the lower the impact.

Circular tunneling affects the response of structures located on the ground.

- The highest response of structures with different floors of structures along the displacement horizon is reported within 5 m of the structure and tunnel.
- Maximum drift of structures with different floors of structures observed along the displacement horizon of 5 m distance between the structure and tunnel.
- All drift and displacement values of the structures have decreased with the tunnel and structure spacing along the horizon.
- The depth of the tunnel has an adverse effect on the response of structures. As the tunnel depth increases, the response of the structures decreases.
- The maximum response of structures is at a depth of 5 m below the surface of the tunnel.
- The highest structural and drift response and tunnel impact is on high-rise structures, and looking at the displacement and drift of the 15-story structure the impact of the tunnel and consequently, the ground surface magnification can be observed.

According to the above mentioned, it can be stated that Tunnel-Soil-Structure interaction is a new issue and challenge in civil engineering and urban construction. Because due to the construction of old structures as well as designing and constructing structures that ignore Tunnel-Soil-Structure interactions in design and construction considerations, according to the results of this study, they will be damaged in case of earthquake. This is important because tunnels, especially subways and subway stations, are located in cities and towns with old textures or high-rise structures. And because in this study the 15-floor structure is in its threshold performance, concerns rise in this issue.

1. Nakamura, S., Yoshida, N., and Iwatate, T. (1996) Damage to Daikai Subway Station During the 1995 Hyogoken-Nambu Earthquake and Its Investigation. Japan Society of Civil Engineers, Committee of Earthquake Engineering, 287-295.
2. Hashash, Y.M.A., Hook, J.J., Schmidt, B., and Yao, J.I. (2001) Seismic design and analysis of underground structures. Tunneling and Underground Space Technology, 16, 247–293.
3. Youd, T.L. and Beckman, C.J. (1996) Highway culvert performance during past earthquakes. National Center for Earthquake Engineering Research, Buffalo. Technical Report NCEER-96-0015.
4. Gizzi, F.T. and Masini, N. (2006) Historical damage pattern and differential seismic effects in a town with ground cavities: a case study from Southern Italy. Engineering Geology, 88, 41-58.
5. Tabatabaiefar HR, Fatahi B, Samali B. Numerical and experimental investiga-tions on seismic response of building frames under influence of soil–structure interaction. Adv Struct Eng 2014; 17(1):109-30
6. Lee, V.W. (1977) on deformations near a circular underground cavity subjected to incident plane SH-waves. Proceedings of the Application of Computer Methods in Engineering Conference. Los Angeles, California, U.S.A., II, 951-62.
7. Lee, V.W. and Trifunac, M.D. (1979) Response of tunnels to incident SH-waves. Journal of Engineering Mechanics Division, 105(4), 643-59.
8. Lee, V.W. (1988) Three-dimensional diffraction of elastic waves by a spherical cavity in an elastic half-space. International Journal of Soil Dynamic and Earthquake Engineering, 7(3), 149-161.

9. Lee, V.W. and Karl, J. (1993) Diffraction of SV waves by underground, circular, cylindrical cavities. International Journal of Soil Dynamic and Earthquake Engineering, 11(8), 445-56.
10. Manoogian, M.E. and Lee, V.W. (1996) Diffraction of SH-waves by sub-surface inclusions of arbitrary shape. Journal of Engineering Mechanics, 122, 122-129.
11. Lee, V W., Chen, S., and Hsu, I.R. (1999) Antiplane diffraction from canyon above a subsurface unlined tunnel. Journal of Engineering Mechanics, 25(6), 668-675.
12. Tabatabaiefar HR, Fatahi B, Samali B. An empirical relationship to determine lateral seismic response of mid-rise building frames under influence of soil– structure interaction. Struct Des Tall Special Build 2014; 23(7):526–48 (Wiley- Blackwell).
13. Tabatabaiefar HR, Massumi A. A simplified method to determine seismic responses of reinforced concrete moment resisting building frames under influence of soil–structure interaction. Soil Dyn Earthq Eng 2010; 30(11): 1259–67 (Elsevier Ltd.).
14. Abate, G., Rossella Massimino, M., (2016), "Numerical modelling of the seismic response of a tunnel–soil–aboveground building system in Catania (Italy)", Bull Earthquake Eng, DOI 10.1007/s10518-016-9973-9.
15. Abate, G., Rossella Massimino, M., (2016), "Parametric analysis of the seismic response of coupled tunnel–soil–aboveground building systems by numerical modelling 2016", Bull Earthquake Eng, DOI 10.1007/s10518-016-9975-7.
16. Pitilakis, K. (2014) Seismic Behavior of Circular Tunnels Accounting for above Ground Structures Interaction Effects. Soil Dynamics and Earthquake Engineering, 67, 1-15. doi:10.1016/j.soildyn.2014.08.009.

17. Smerzini, C., Aviles, J., Sanchez-Sesma, F.J, and Paolucci, R. (2009) Effect of Underground Cavities on Surface Earthquake Ground Motion under SH Wave Propagation. Earthquake Engineering and Structural Dynamics, 32(12), 1441-1460.
18. Huai-feng Wang, Meng-lin Lou, Ru-lin Zhang – 2017- "Influence of presence of adjacent surface structure on seismic response of underground structure". Soil Dynamics and Earthquake Engineering 100 (2017) 131–143. http://dx.doi.org/10.1016/j.soildyn.2017.05.031.
19. Yiouta-Mitra, P., Kouretzis, G., Bouckovalas, G., and Sofianos, A. (2007) Effect of underground structures in earthquake resistant design of surface structures. Dynamic Response and Soil Properties. Geo-Denver: New Peaksin Geotechnics.
20. Baziar, M.H., Rabeti Moghadam, M., Kim, D.S., and Choo, Y.W. (2014) Effect of underground tunnel on the ground surface acceleration. Tunneling and Underground Space Technology, 44, 10-22.
21. Rostami, A., Asghari, N., Ziarati, M. A., Jahani, S., & Shahi, B. (2016). Investigating Effect of Tunnel Gate Shapes with Similar Cross Section on Inserted Forces on Its Coverage and Soil Surface Settlement. Open Journal of Civil Engineering, 6(03), 358–369. doi:10.4236/ojce.2016.63030.
22. Tsinidis Grigorios – 2013 - EXPERIMENTAL AND NUMERICAL INVESTIGATION OF THE SEISMIC BEHAVIOR OF RECTANGULAR TUNNELS IN SOFT SOILS - Computational Methods in Structural Dynamics and Earthquake Engineering.
23. Hamid Reza Tabatabaiefar, Behzad Fatahi. 2014 - Idealization of soil–structure system to determine inelastic seismic response of mid-rise building frames. Soil Dynamics and Earthquake Engineering 66 (2014) 339–351 http://dx.doi.org/10.1016/j.soildyn.2014.08.007.

24. Fatahi Behzad – 2014 - Fully Nonlinear versus Equivalent Linear Computation Method for Seismic Analysis of Midrise Buildings on Soft Soils - International Journal of Geomechanics - ASCE, ISSN 1532-3641/04014016(15).
25. Rostami, A., Alielahi, H., Zare, M., & Haghighi, K. (2016). Frequency and Surface Slopes Effects on the Surface Displacement by Drilling Shallow and Deep Tunnels under Dynamic Loads. Open Journal of Marine Science, 6(03), 353–370. doi:10.4236/ojms.2016.63030.
26. Sica Stefania – 2013 - Ground motion amplification due to shallow cavities in nonlinear soils - Springer Science - DOI 10.1007/s11069-013-0989-z.
27. Tsaur Deng-How – 2012 - MULTIPLE SCATTERING OF SH WAVES BY AN EMBEDDED TRUNCATED CIRCULAR CAVITY - Journal of Marine Science and Technology - Vol. 20, No. 1, pp. 73-81.
28. Liu Qijian – 2013 - Scattering of plane P, SV or Rayleigh waves by a shallow lined tunnel in an elastic half space – Elsevier - 10.1016/j.soildyn.2013.02.007.
29. Luzhen Jiang – 2010 - Seismic response of underground utility tunnels: shaking table testing and FEM analysis - EARTHQUAKE ENGINEERING AND ENGINEERING VIBRATION - Vol.9, No.4.
30. Rostami, A., Ziarati, M. A., Shahi, B., & Jahani, S. (2016). Evaluation of Seismic Behavior and Earth's Surface Acceleration, by Interaction of Tunnels with Different Shapes and Different Types of Soils. Open Journal of Civil Engineering, 6(02), 242–253. doi:10.4236/ojce.2016.62022.
31. Rostami, A., Dehkordi, P. K., Ziarati, M. A., Jahani, S., & Lotfi, K. (2016). The Types of Tunnels Maintenance in Umbrella Arch Method. Open Journal of Civil Engineering, 6(02), 156–162. doi:10.4236/ojce.2016.62014.

32. Rostami, A., Firoozfar, A., Adhami, B., & Asghari, N. (2016). Impact of Soil Type Used in Tunneling on Land Subsidence and Mobility Effective Time under Different Earthquake Records. Open Journal of Geology, 6(11), 1469–1480. doi:10.4236/ojg.2016.611104.
33. Arash Rostami, Hamid Alielahi, Abdoreza Sarvghad Moghadam, Mahmood Hosseini. Steel Buildings' Seismic and Interaction Behavior, Under Different Shapes of Tunnel Drilling. International Journal of Geotechnical Earthquake Engineering. Volume 7 • Issue 2 • July-December 2016. DOI: 10.4018/IJGEE.2016070101.
34. Behzad Fatahi, Aslan S. Hokmabadi, and Bijan Samali. Seismic Performance Based Design for Tall Buildings Considering Soil-Pile-Structure Interaction. Advances in Soil Dynamics and Foundation Engineering GSP 240. ASCE 2014.
35. BHRC, Iranian Code of Practice for Seismic Resistance Design of Buildings, Standard no. 2800 (3rd edition), Building and Housing Research Center (2005).
36. ASCE/SEI 7-05, Minimum Design Loads for Buildings and Other Structures.
37. Standard No. 519, Part 6, Iranian National Building Code for Structural Loadings, Ministry of Housing and Urban Development, Tehran, Iran (2004).
38. Kuhlemeyer R.L. and Lysmer J. (1973) Finite element method accuracy for wave propagation problems. Journal of Soil Mechanics and Foundations, ASCE, 99(SM5), 421-427.
39. Kramer SL. Geotechnical earthquake engineering. Prentice Hall Civil Engineering and Engineering Mechanics Series; 1996.
40. ABAQUS Software. V 6.14.2.

41. ATC-40. Seismic Evaluation and Retrofit of Concrete Buildings. Applied Technology Council, Seismic Safety Commission, State of California; 1996.
42. Vision 2000 Committee. Performance Based Seismic Engineering of Buildings. Sacramento, CA: Structural Engineers Association of California (SEAOC); 1995.
43. FEMA 440. NEHRP Recommended Provisions for Improvement of Nonlinear Static Seismic Analysis Procedures, ATC-55 Project. Washington, DC: Emergency Management Agency; 2005
44. Conniff DE, Kiousis PD. Elasto-plastic medium for foundation settlements and monotonic soil–structure interaction under combined loadings. Int J Numer Anal Methods Geomech 2007; 31:789–807.
45. Rayhani MH, El Naggar MH. Numerical modelling of seismic response of rigid foundation on soft soil. Int J Geomech 2008; 8(6):336–46.
46. Itasca Consulting Group. FLAC2D: fast lagrangian analysis of continua, version 6.0. User's manual. Minneapolis; 2008.
47. Cundall PA, Hart RD. Numerical modeling of discontinued. Eng Comput 1992; 9: 101–13.
48. Chopra AK, Gutierres JA. A substructure method for earthquake analysis of structures including structure–soil interaction. Earthq Eng Struct Dyn 1978; 6(1):51–69.
49. Roesset JM, Ettouney MM. Transmitting boundaries: a comparison. Int J Numer Anal Methods Geomech 1977; 1:151–76.
50. Lysmer J, Kuhlemeyer RL. Finite dynamic model for infinite media. J Eng Mech Div ASCE 1969; 95(6):859–77.
51. Kocak S, Mengi Y. A simple soil–structure interaction model. Appl Math Model 2000; 24(8–9):607–35.
52. Dutta CH, Roy R. A critical review on idealization and modelling for interaction among soil–foundation–structure system. Comput Struct 2002; 80(3): 1579–94.

53. Zheng J, Takeda T. Effects of soil–structure interaction on seismic response of PC cable-stayed bridge. Soil Dyn Earthq Eng 1995; 14(6):427–37.
54. Koutromanos IA, Maniatakis CHA, Spyrakos CC. Soil–structure interaction effects on base-isolated buildings founded on soil stratum. Eng Struct 2009; 31(3):729–37.
55. NEHRP Recommended Provisions for Seismic Regulation for New Buildings and Other Structures (FEMA 450). Washington, DC, Edition: Federal Emergency Management Agency; 2003.
56. Luco JE, Hadjian AH. Two dimensional approximations to the three-dimensional soil–structure interaction problem. Nucl Eng Des 1974; 31: 195–203.
57. Zhang X, Wegner JL, Haddow JB. Three-dimension dynamic soil–structure interaction analysis in the time domain. Earthq Eng Struct Dyn 1999; 28: 1501–24.
58. Seo CG, Yuna CB, Kimb JM. Three-dimensional frequency-dependent infinite elements for soil–structure interaction. Eng Struct 2007; 29:3106–20.
59. Galal K, Naimi M. Effect of conditions on the response of reinforced concrete tall structures to near fault earthquakes. Struct Design Tall Special Build 2008; 17(3):541–62.
60. Tabatabaiefar HR, Fatahi B, Samali B. Numerical and experimental investigations on seismic response of building frames under influence of soil–structure interaction. Adv Struct Eng 2014; 17(1):109–30.